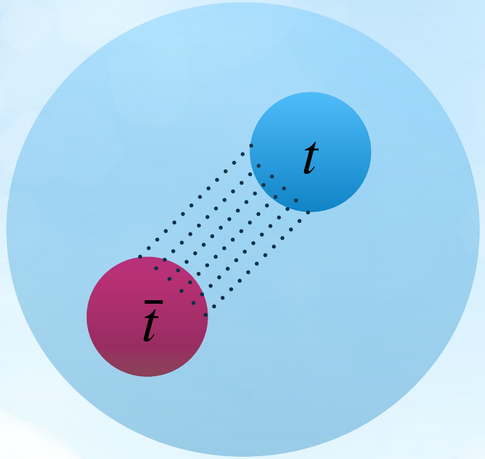
大阪大学
THE UNIVERSITY OF OSAKA

International College



Toponium at the ILC revisited

Ya-Juan Zheng
The University of Osaka

International Workshop on Future Linear Colliders 2026

KEK
November 12, 2026

Based on works with B. Fuks, K. Hagiwara, J.Kanzaki, K.Ma, L. Munoz and H.Shao.



大阪大学「ワニ博士」

Outline

- ~1990, early works on toponium.
- 2017 $e^+e^- \to t\bar{t}H$ @ ILC, density matrix for $t\bar{t}$ spin correlations.
- 2019, hint of anomaly in LHC run 2 data.
- 2021, toponium gives dileptons with small $\phi(ll'), m(ll')$.
- 2025, both ATLAS and CMS confirmed that observed anomaly is consistent with toponium formation.
- 2026, we revisit $e^+e^- \to \Theta + \chi_t^1$.
- Quantum physics @ 10^{-7} times the atomic scale.

Early works on toponium

- Late 1980's: $m_t > 100\ GeV \rightarrow \Gamma_t \sim \mathcal{O}(1)\ GeV \rightarrow$ no sharp resonances

- 1987: All toponiums have the same decay width, $2\Gamma_t$,
  Green's function $(E + i\Gamma_t - H)G(E;\vec{r}) = \delta^3(\vec{r})$
  by V.S.Fadin and V.A. Khoze, JETP Lett 46, 417 (1987)

- 1991: Numerical solution of G(E;0) for QCD potential,
  by M.Strassler and M.Peskin, PRD43, 1500 (1991)

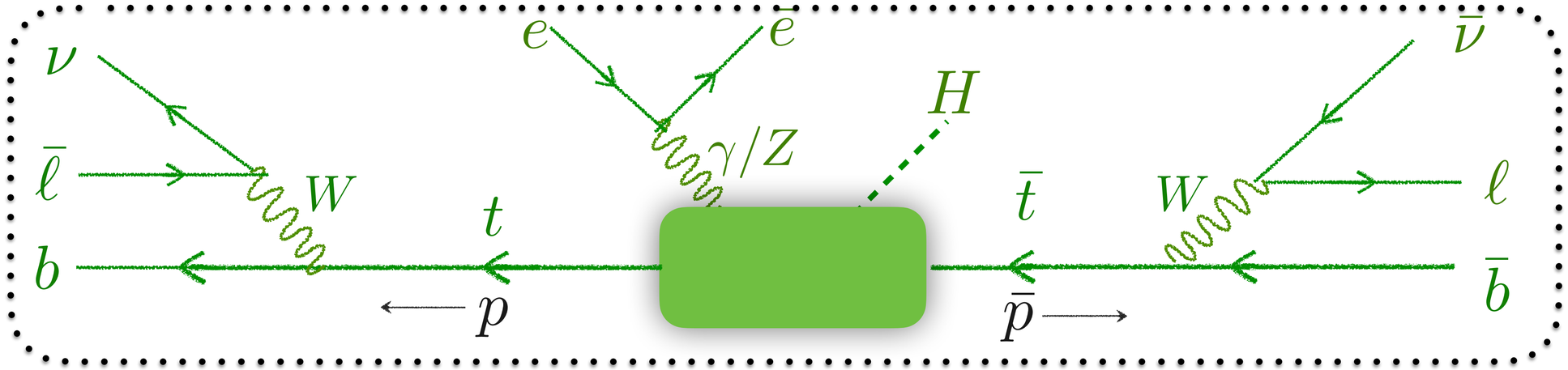
- 1992: Fourier transform $\tilde{G}(E;p) \rightarrow$ momentum distributions
  by Y. Sumino, K.Fujii, K.Hagiwara, H. Murayama, C.K.Ng, PRD47, 56(1993).

- 1992: S- and P- wave interference gives A_{FB} in $e^+e^- \rightarrow t\bar{t}$
  by H. Murayama, and Y.Sumino, PRD47,82 (1993).

- 1992: $\tilde{G}(E;p)$ directly from solving Lipman-Schwinger equation,
  by M. Jezebek, J.H.Kuhn, T.Teubner, ZPC56, 653 (1992).

2017 $e^-e^+ \to t\bar{t}H$

We studied $e^-e^+ \to t\bar{t}H$ including toponium contributions.



Decay final states keep all the spin correlations of $t\bar{t}$.

$$\mathcal{M} = \bar{u}(\nu)\gamma^\mu P_L v(\bar{\ell}) \frac{-g_{\mu\nu}}{q^2 - m_W^2} \bar{u}(b)\gamma^\nu P_L \frac{\not{p} + m_t}{p^2 - m_t^2} \quad \frac{m_t - \not{\bar{p}}}{\bar{p}^2 - m_t^2} \gamma^\rho P_L v(\bar{b}) \frac{-g_{\rho\sigma}}{q'^2 - m_W^2} \bar{u}(\ell)\gamma_\sigma P_L v(\bar{\nu})$$

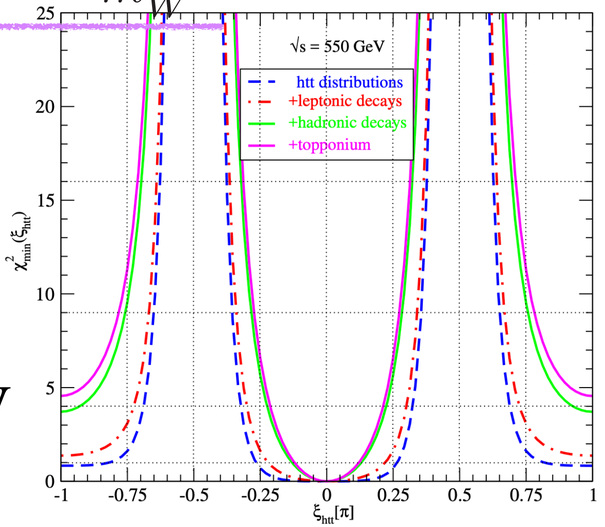
$$= \sum_{h,\bar{h}} \underbrace{\frac{u_L^\dagger(\nu)\sigma_-^\mu v_L(\bar{\ell})}{q^2 - m_W^2} \frac{u_L^\dagger(b)\sigma_{-\mu} u_L(p,h)}{p^2 - m_t^2}}_{\mathcal{T}_h^{t\to b\bar{\ell}\nu}} \underbrace{\bar{u}(p,h) \quad v(\bar{p},\bar{h})}_{\hat{\mathcal{M}}_{h\bar{h}}} \underbrace{\frac{v_L^\dagger(\bar{p},h)\sigma_-^\rho v_L(\bar{b})}{\bar{p}^2 - m_t^2} \frac{u_L^\dagger(\ell)\sigma_{-\rho} v(\bar{\nu})}{q'^2 - m_W^2}}_{\bar{\mathcal{T}}_{\bar{h}}^{\bar{t}\to\bar{b}\ell\bar{\nu}}}$$

$$|\mathcal{M}|^2 = \sum_{h,\bar{h}} \sum_{h',\bar{h}'} \underbrace{(\mathcal{T}_h)(\mathcal{T}_{h'})^*}_{\rho_{hh'}^{t\to b\bar{\ell}\nu}} \underbrace{(\hat{\mathcal{M}}_{h\bar{h}}\hat{\mathcal{M}}_{h'\bar{h}'})^*}_{\rho_{h\bar{h},h'\bar{h}'}^{X\to t\bar{t}}} \underbrace{(\bar{\mathcal{T}}_{\bar{h}})(\bar{\mathcal{T}}_{\bar{h}'})^*}_{\rho_{\bar{h}\bar{h}'}^{\bar{t}\to\bar{b}\ell\bar{\nu}}}$$

Sum of all helicity ≡ Trace of density matrices.

Production is process dependent.

$$\sqrt{s} = 550 \text{ GeV}$$



[K.Hagiwara, H.Yokoya, and YJZ JHEP02 (2018), arXiv:1712.09953]

t and $\bar{t}$ decay

$$\mathcal{T}_h^{t\to b\bar{\ell}\nu} \sim u_L^\dagger(\nu)\sigma_-^\mu v_L(\bar{\ell})u_L^\dagger(b)\sigma_{-\mu}u_L(p,h)$$
$$= u_L^*(\nu)_i(\sigma_-^\mu)_{ij}u_L(\bar{\ell})_j u_L^*(b)_k(\sigma_{-\mu})_{k\ell}u_L(p,h)_\ell$$
$$= 2\ \underbrace{u_L^\dagger(\nu)(i\sigma^2)u_L^*(b)}_{\sim m_{\nu b}}\ \underbrace{u_L(\bar{\ell})^T(i\sigma^2)u_L(p,h)}_{\sim\sqrt{2E_{\bar{\ell}}m_t}\cos\frac{\theta^*}{2}}$$

$$\sigma_\pm^\mu = (1, \pm\vec{\sigma})$$

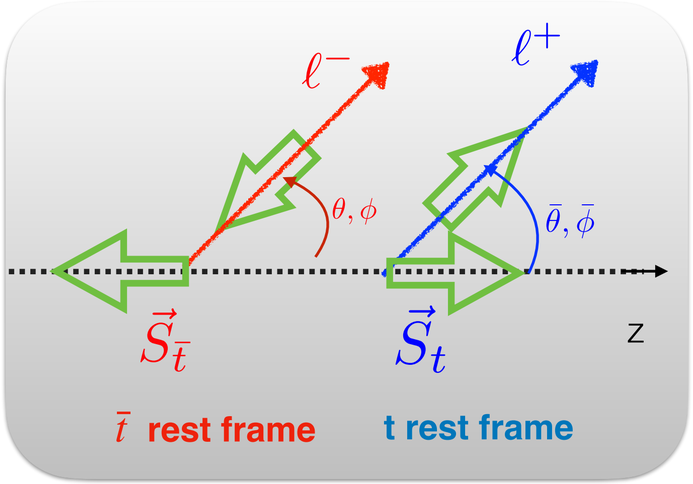
$$(\sigma_\pm^\mu)_{k\ell}(\sigma_{\pm\mu})_{mn} = 2(i\sigma^2)_{km}(i\sigma^2)_{\ell n}$$

Fierz Identity

in the top rest frame

$$\mathrm{d}\rho_{hh'}^{t\to\bar{\ell}} = B(t\to b\bar{\ell}\nu)\begin{pmatrix} 1+\cos\bar{\theta}^* & \sin\bar{\theta}^* e^{i\bar{\phi}^*} \\ \sin\bar{\theta}^* e^{-i\bar{\phi}^*} & 1-\cos\bar{\theta}^* \end{pmatrix}\frac{d\cos\bar{\theta}^* d\bar{\phi}^*}{4\pi}$$

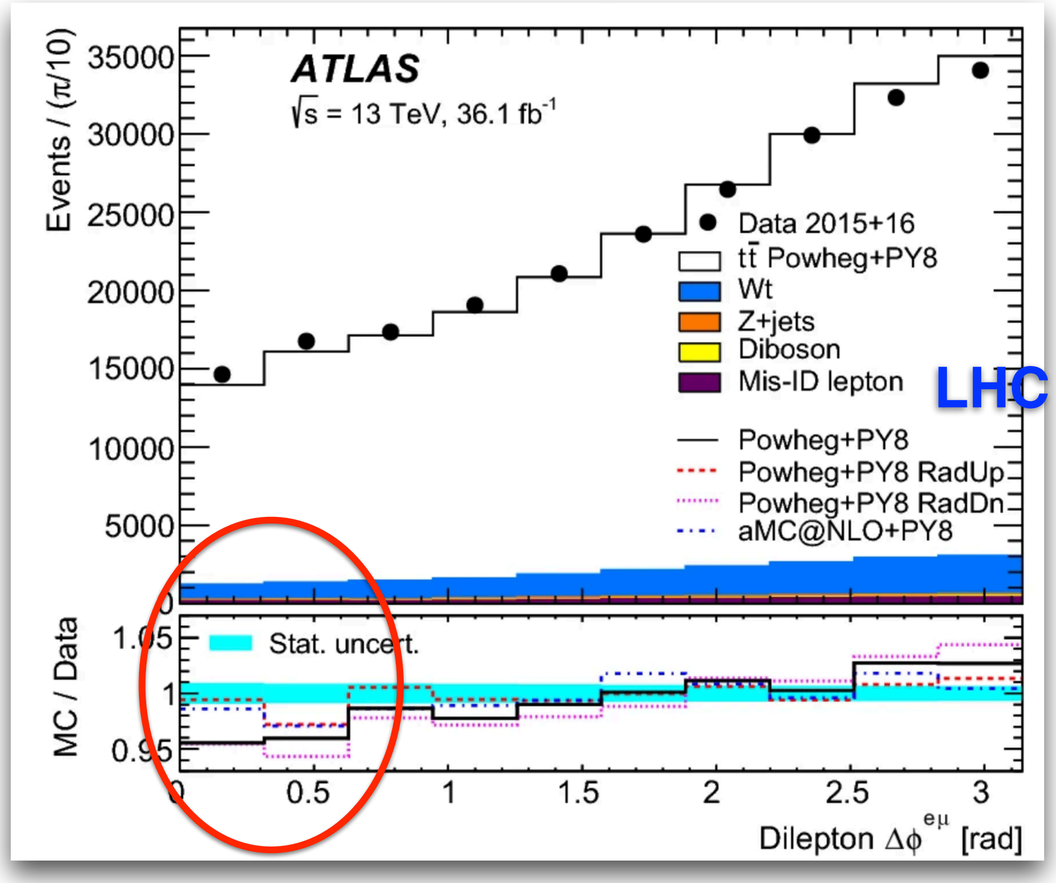
$$\mathrm{d}\bar{\rho}_{\bar{h}\bar{h}'}^{\bar{t}\to\ell} = B(\bar{t}\to\bar{b}\ell\bar{\nu})\begin{pmatrix} 1+\cos\theta^* & \sin\theta^* e^{-i\phi^*} \\ \sin\theta^* e^{i\phi^*} & 1-\cos\theta^* \end{pmatrix}\frac{d\cos\theta^* d\phi^*}{4\pi}$$



Appendix A in [K.Hagiwara, H. Yokoya, and YJZ, JHEP2018, 1712.09953] gives $t\to b\bar{\ell}\nu$ and $b\bar{d}u$ decay density matrices. The above forms are obtained after integrating over $b+\nu$ phase space. Hadronic decays are also sensitive to top spin, because one of W-decay dijets gives the same information as the charged leptons in semi-leptonic decays.

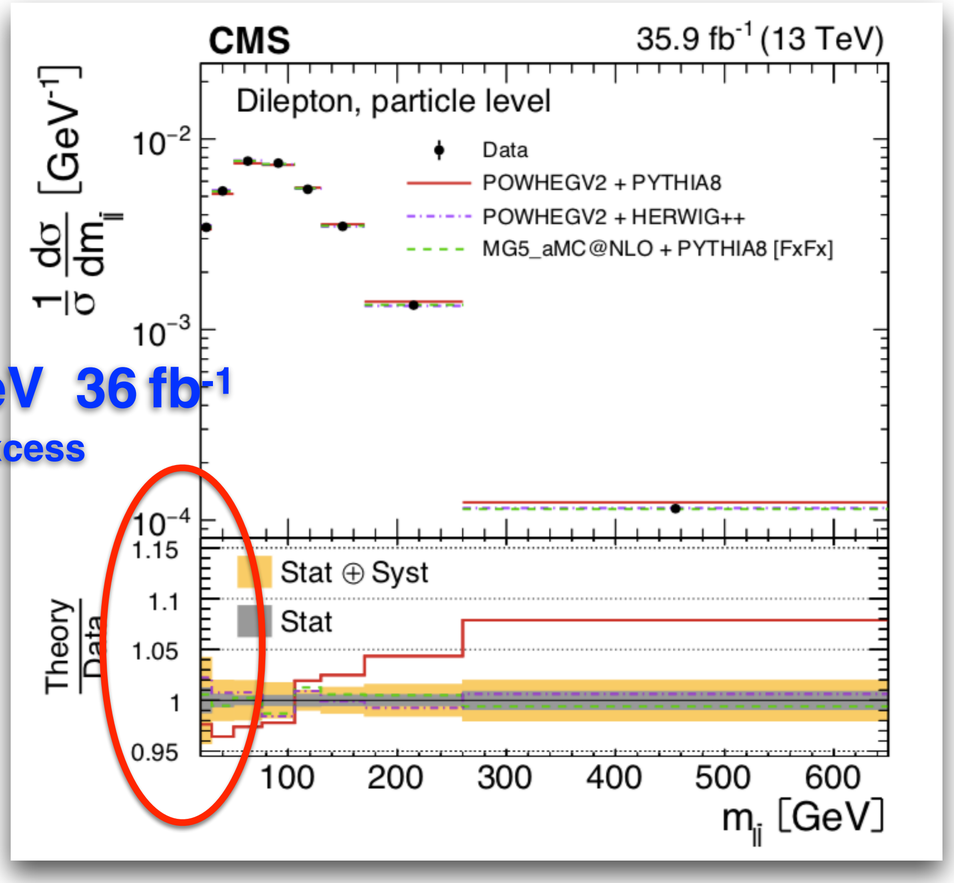
2019 Anomaly?

2019 LHC run2 data for $t\bar{t}$ production cross section and dilepton events at $\sqrt{s} = 13$ TeV, ~ 36 fb^{-1}.



LHC 13TeV 36 fb^{-1}

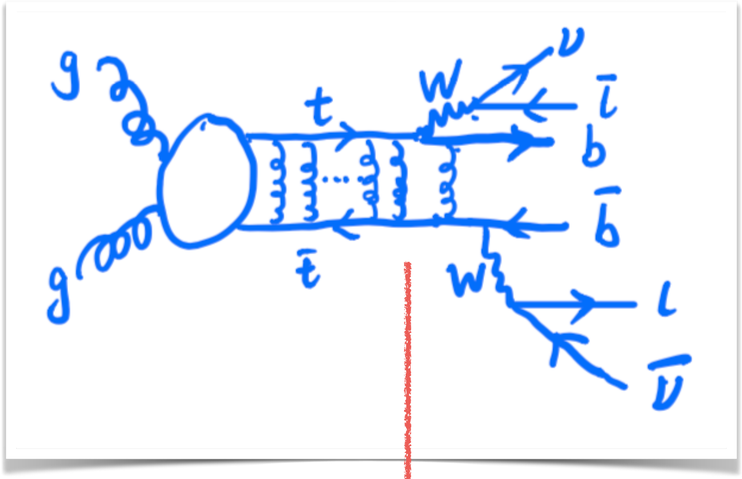
~3σ excess



[ATLAS EPJC2020]

[CMS JHEP2019]

- **Both ATLAS and CMS observed excess of data over the 'SM' prediction at low ϕ(ll'), m(ll') bins [ATLAS EPJC 2020, CMS JHEP 2019].**
  - **This may suggest that either $t\bar{t}$ production MC underestimates small angle dileptons, or new physics.**
  - **The standard $t\bar{t}$ MC does not contain toponium.**

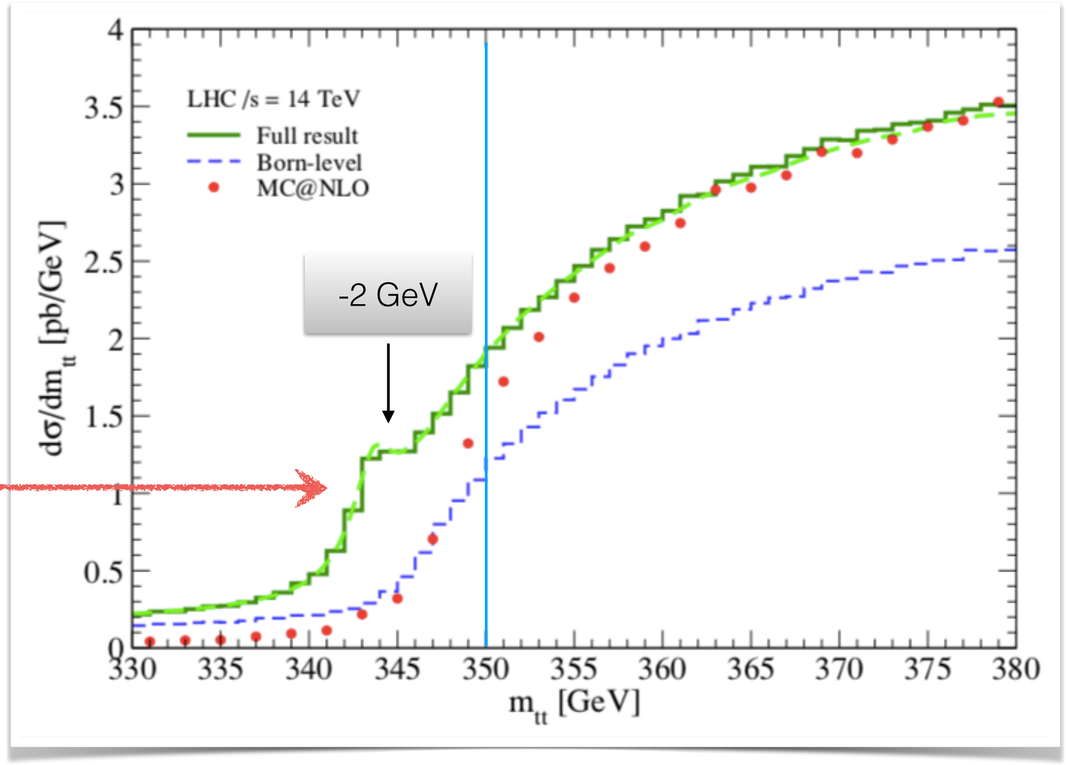


NRQCD Hamiltonian

$$\left[(E+i\Gamma_t)-\left\{-\frac{\nabla^2}{m_t}+V_{\rm QCD}^{(c)}(r)\right\}\right]G^{(c)}(E+i\Gamma_t,\vec{r})=\delta^3(\vec{r})$$

$$\tilde{G}^{(c)}(E+i\Gamma_t,\vec{p})=\int d^3\vec{r}e^{-i\vec{p}\cdot\vec{r}}G^{(c)}(E+i\Gamma_t,\vec{r})$$

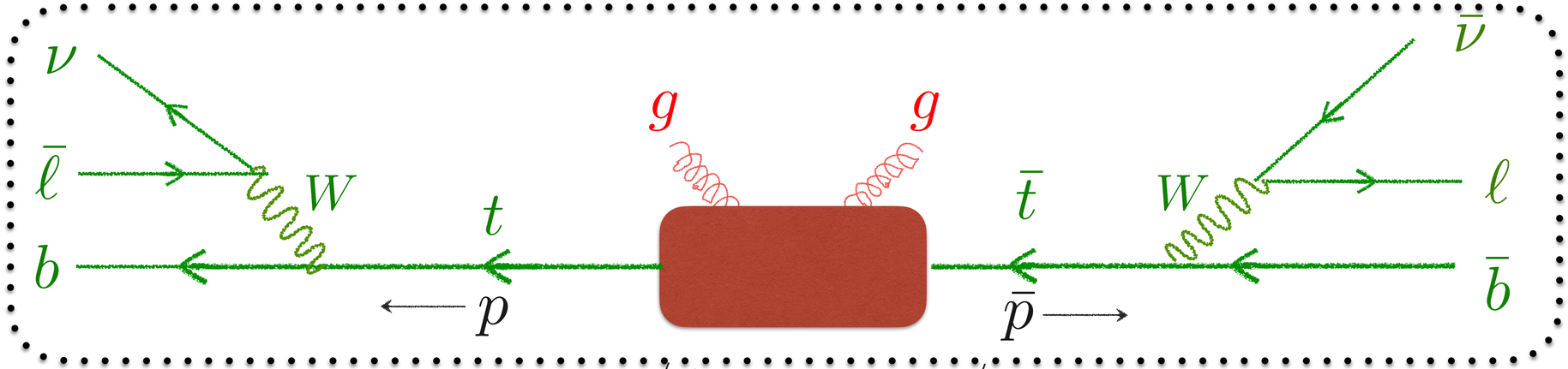
$$|\mathcal{M}|^2\rightarrow\left|\mathcal{M}\frac{\tilde{G}(E;p^*)}{\tilde{G}_0(E;p^*)}\right|^2$$



✳ Multiple gluon exchange effects are evaluated by using Green's function of the non-relativistic Hamiltonian with QCD potential. [V.S.Fadin and V.A.Khoze (JETP1987) (Sov. J. Nucl. Phys1988)]

[Y.Sumino and H.Yokoya, JHEP2010]

2020



$$\mathcal{M} = \bar{u}(\nu)\gamma^\mu P_L v(\bar{\ell}) \frac{-g_{\mu\nu}}{q^2 - m_W^2} \bar{u}(b)\gamma^\nu P_L \frac{\not{p} + m_t}{p^2 - m_t^2} \quad \frac{m_t - \not{\bar{p}}}{\bar{p}^2 - m_t^2} \gamma^\rho P_L v(\bar{b}) \frac{-g_{\rho\sigma}}{q'^2 - m_W^2} \bar{u}(\ell)\gamma_\sigma P_L v(\bar{\nu})$$

$$= \sum_{h,\bar{h}} \mathcal{T}_h^{t\to b\bar{\ell}\nu} \hat{\mathcal{M}}_{h\bar{h}} \bar{\mathcal{T}}^{\bar{t}\to\bar{b}\ell\bar{\nu}}$$

$$|\mathcal{M}|^2 \sim \sum_{h,\bar{h}} \sum_{h',\bar{h}'} \rho_{h,h'}^{t\to b\bar{\ell}\nu}(\bar{\theta},\bar{\phi}) \rho_{h\bar{h},h'\bar{h}'}^{gg\to t\bar{t}} \rho_{\bar{h}\bar{h}'}^{\bar{t}\to\bar{b}\ell\bar{\nu}}(\theta,\phi)$$

$$\rho_{h\bar{h},h'\bar{h}'}^{gg\to t\bar{t}} = \hat{M}_{h\bar{h}} \hat{M}^*_{h'\bar{h}'} = \begin{pmatrix} \rho_{++,++} & \rho_{++,--} \\ \rho_{--,++} & \rho_{--,--} \end{pmatrix} = \frac{1}{2} \begin{pmatrix} 1 & -1 \\ -1 & 1 \end{pmatrix}$$ production density matrix

$$\sum_{h\bar{h}} \sum_{h'\bar{h}'} \rho_{h\bar{h},h'\bar{h}'} \rho_{hh'}^{t\to\ell^+}(\bar{\theta},\bar{\phi}) \rho_{\bar{h}\bar{h}'}^{\bar{t}\to\ell^-}(\theta,\phi) = F(\bar{\theta},\bar{\phi};\theta,\phi)$$

$$= \frac{1+\cos\bar{\theta}}{2}\frac{1+\cos\theta}{2} + \frac{1-\cos\bar{\theta}}{2}\frac{1-\cos\theta}{2} + \frac{1}{2}\sin\bar{\theta}\sin\theta\cos(\bar{\phi}-\phi)$$

= 1
when $(\theta,\phi) = (\bar{\theta},\bar{\phi})$

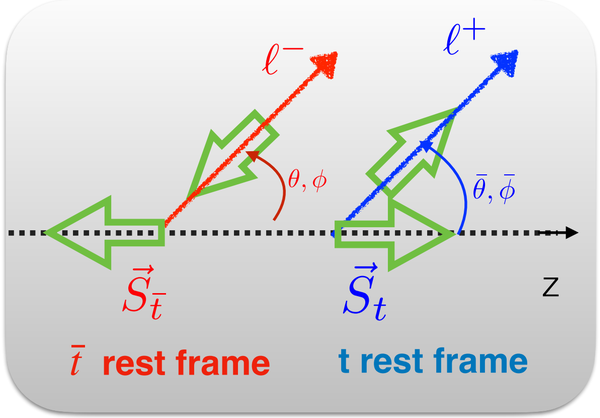
$p^* \to 0$

$$\frac{1+\cos\theta_{\ell^+\ell'^-}}{2}$$

$$\hat{\mathcal{M}}_{-,-} = -\hat{\mathcal{M}}_{+,+}$$

from

$$|\eta_t> = \frac{|\uparrow>_t |\downarrow>_{\bar{t}} - |\downarrow>_t |\uparrow>_{\bar{t}}}{\sqrt{2}}$$



[B.Fuks, K.Hagiwara, K.Ma and YJZ. Phys.ReV.D104(2021)3,034023, Eur.Phys.J.C85(2025) 2, 157]

Predictions based on LHC 36/fb analysis

2021

Cut	$t\bar{t}$	Toponium	Ratio
Initial	113,000,000	900,000	0.0079
Di-lepton	5,160,000	41,000	0.0079
$p_T, \lvert\eta\rvert, \Delta R$	1,370,000	10,300	0.0075
$\Delta\varphi_{\bar{\ell}\ell'}$	178,000	4,060	0.023
$m_{\bar{\ell}\ell'}$	77,000	2,760	0.036
$m_T(\bar{\ell}\ell' b\bar{b}; \nu_\ell \bar{\nu}_{\ell'})$	40,800	2,460	0.060
$t\bar{t}$ kinematical fit	20,400	1,420	0.070

$\sqrt{s} = 13$ TeV

$140\ \text{fb}^{-1}$

$m_t = 173$ GeV

$p_T > 25$ GeV

$|\eta| < 2.5$

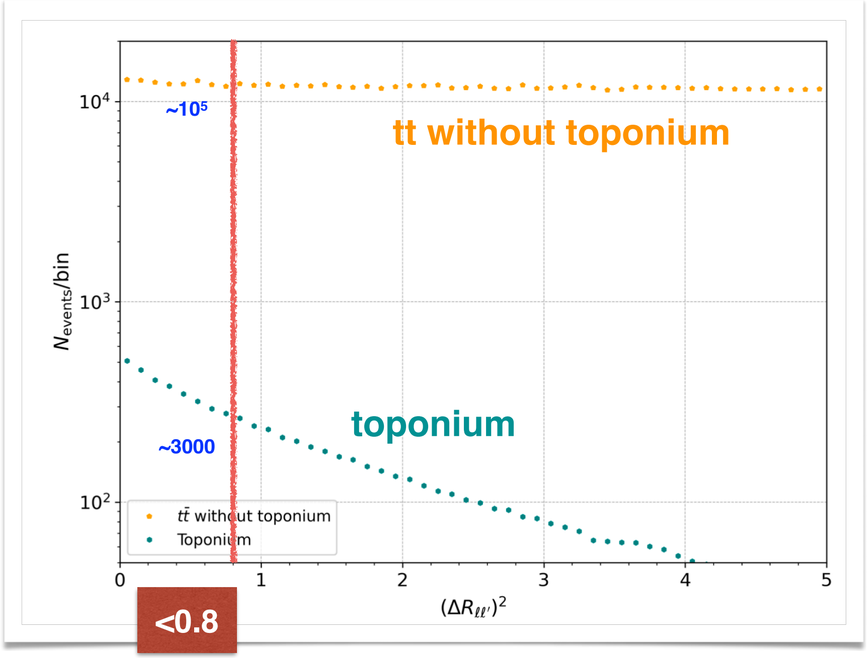
$\Delta R > 0.4$

$m_T(\bar{\ell}\ell' b\bar{b}; \nu_\ell \bar{\nu}_{\ell'}) < 320$ GeV

< 0.8%

7%

2024



$$(\Delta R_{\ell\ell'})^2 = (\Delta\phi_{\ell\ell'})^2 + (\Delta\eta_{\ell\ell'})^2$$ <0.8

$$\frac{S}{B} \sim 3\%$$

$$\frac{S}{\sqrt{B+S}} \to \frac{S}{\sqrt{B}} \sim \frac{3000}{\sqrt{10^5}} \sim 9$$

Toponium study starts!

[1] B.Fuks, K.Hagiwara, Kai Ma and YJZ, 'Signatures of toponium formation in LHC run 2 data', Phys. Rev.D 104 (2021) 3, 034023.
[2] B.Fuks, K.Hagiwara, Kai Ma and YJZ, 'Simulating toponium formation signals at the LHC', arXiv:2411.18962. EPJC 85 (2025) 157.

Next steps

- P-wave toponium

$gg \to (t\bar{t})_{\text{color singlet}}$ → LHC physics

η_t', χ_t^0, χ_t^2 are almost degenerate and interfere.

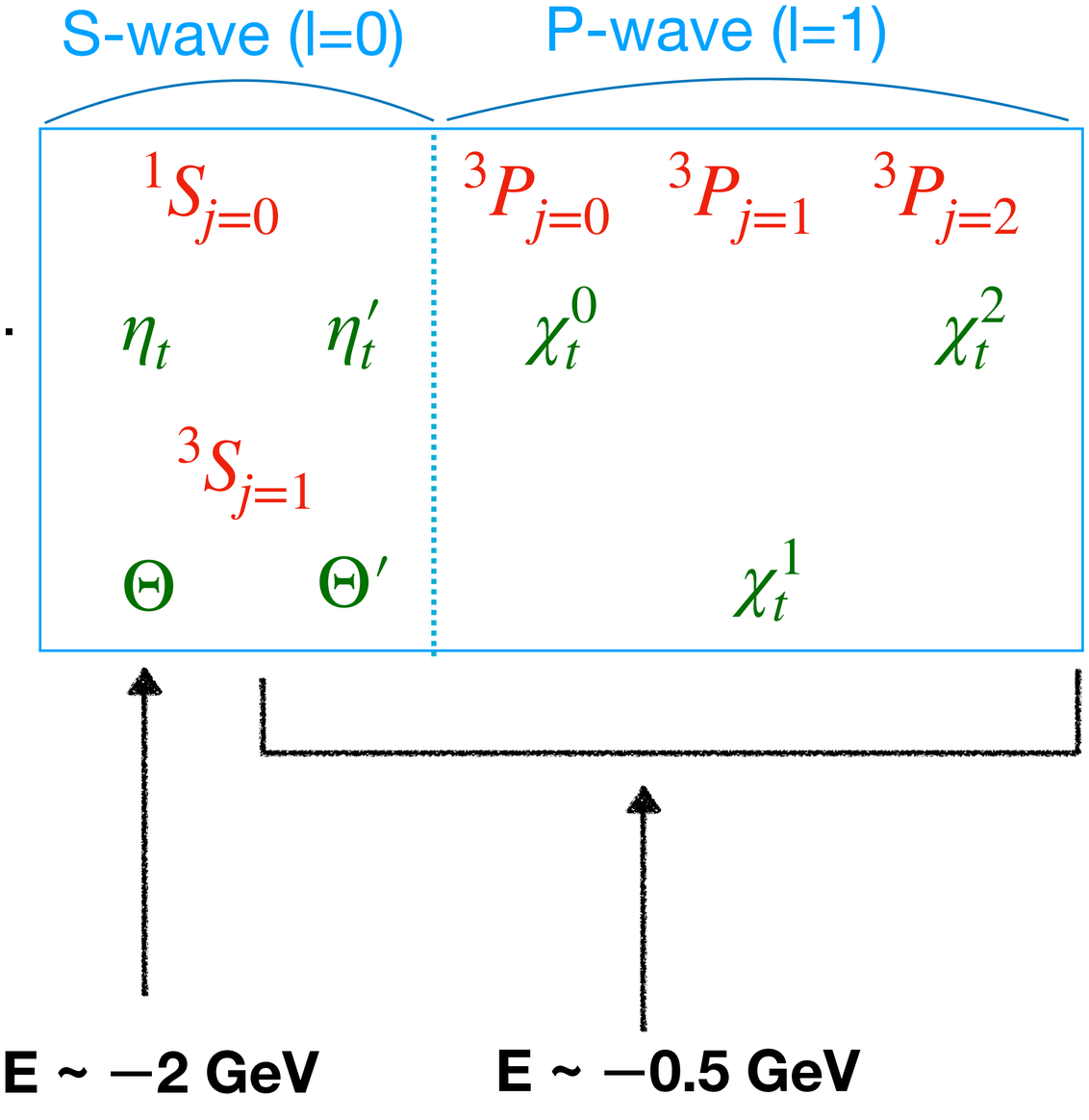
- Spin-1 toponium

$q\bar{q} \to (t\bar{t})_{\text{color singlet}}$ → HL-LHC? $e^+e^- @ \sqrt{s} \approx 2m_t$

- Merging of NRQCD and QCD @ NLO

Our current simulation program has a discontinuity $@m(t\bar{t}) = 2m_t + 4\text{GeV}$.
Experts help needed.

- Precise measurement of m_t @ LHC



dilepton angular distributions

- η_t, η_t' are spin singlets → Prefers $\theta_{\ell\bar{\ell}} \approx 0$

=1 when $(\bar{\theta}, \bar{\phi}) = (\theta, \phi)$

$$\frac{\uparrow\downarrow - \downarrow\uparrow}{\sqrt{2}} \quad \frac{1}{2}\begin{pmatrix} 1 & -1 \\ -1 & 1 \end{pmatrix} \quad \text{production density matrix}$$

$$\rightarrow \frac{1+\cos\bar{\theta}}{2}\frac{1+\cos\theta}{2} + \frac{1-\cos\bar{\theta}}{2}\frac{1-\cos\theta}{2} + \frac{1}{2}\sin\bar{\theta}\sin\theta\cos(\bar{\phi}-\phi)$$

- Θ, $\chi_t^{0,1,2}$ are all spin triplets → Prefers $\theta_{\ell\bar{\ell}} \approx \pi$

$$\uparrow\uparrow \quad \begin{pmatrix} 1 & 0 \\ 0 & 0 \end{pmatrix} \rightarrow \frac{(1+\cos\bar{\theta})(1-\cos\theta)}{2}$$

largest when $(\bar{\theta}, \theta) = (0,\pi)$

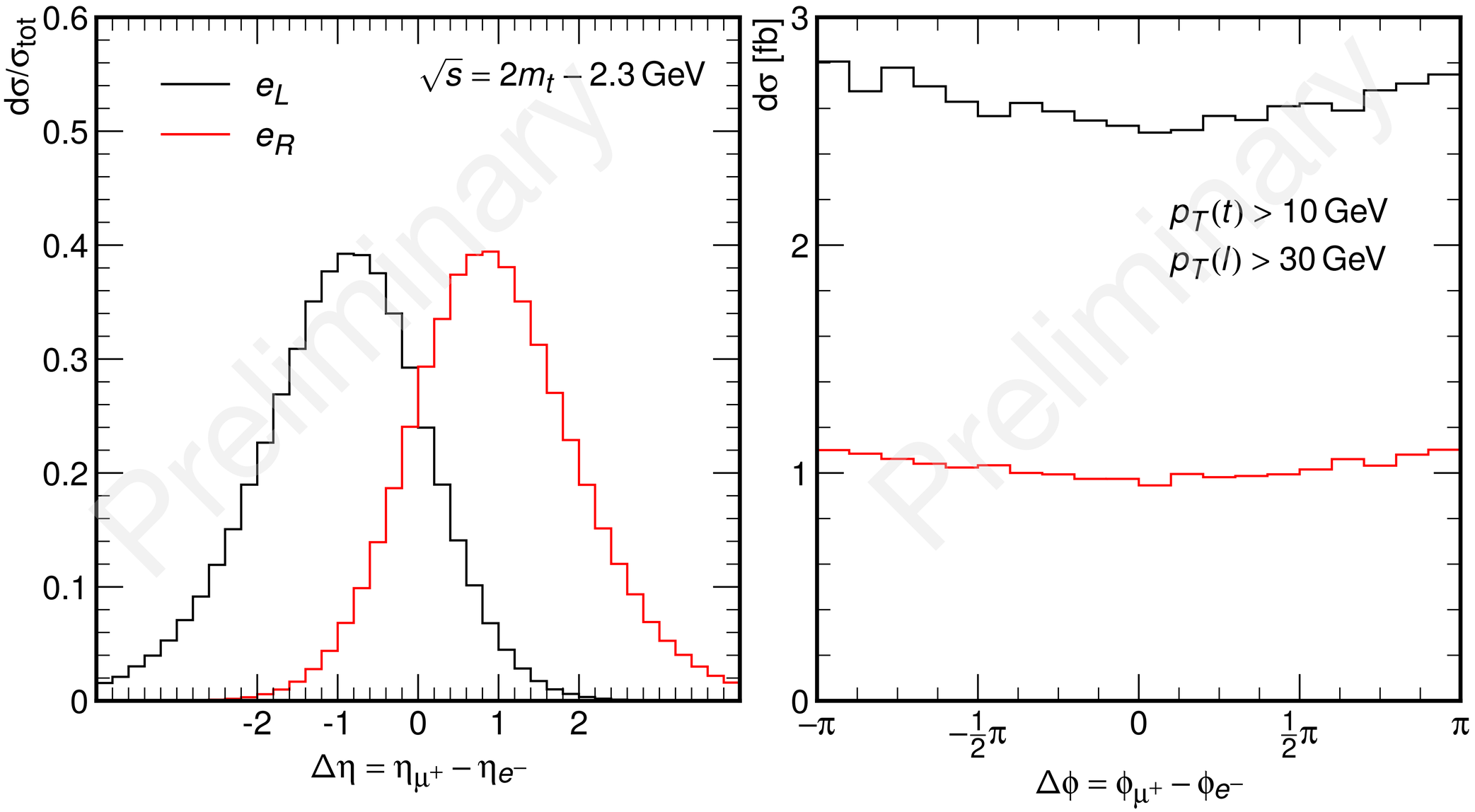
$$\frac{\uparrow\downarrow + \downarrow\uparrow}{\sqrt{2}} \quad \frac{1}{2}\begin{pmatrix} 1 & 1 \\ 1 & 1 \end{pmatrix} \rightarrow \frac{1+\cos\bar{\theta}}{2}\frac{1+\cos\theta}{2} + \frac{1-\cos\bar{\theta}}{2}\frac{1-\cos\theta}{2} - \frac{1}{2}\sin\bar{\theta}\sin\theta\cos(\bar{\phi}-\phi)$$

largest when $\bar{\phi} - \phi = \pi$

$$\downarrow\downarrow \quad \begin{pmatrix} 0 & 0 \\ 0 & 1 \end{pmatrix} \rightarrow \frac{(1-\cos\bar{\theta})(1+\cos\theta)}{2}$$

largest when $(\bar{\theta}, \theta) = (\pi,0)$

$e^+e^- \to t\bar{t} \to \mu^+\nu_\mu b + e^-\bar{\nu}_e\bar{b}$ $m_t = 172.5\,\text{GeV}$, $\Gamma_t = 1.315\,\text{GeV}$

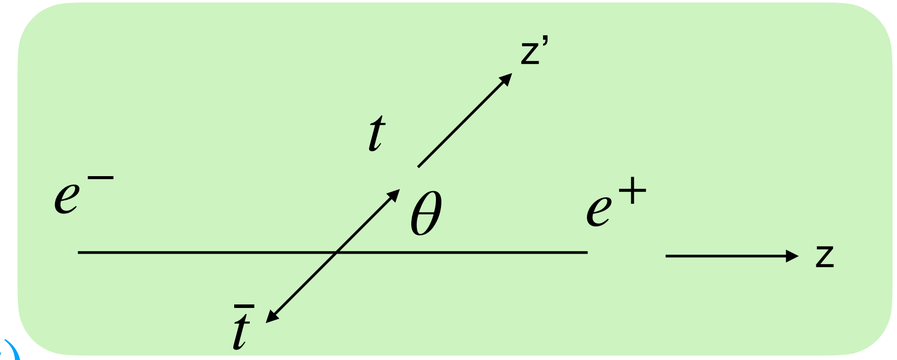


Preliminary

Helicity amplitudes for $e^-e^+ \to t\bar{t}$ revisited

$$M_\alpha^{\sigma\bar{\sigma}} = M\left(e^-(k,\frac{\alpha}{2})e^+(\bar{k},-\frac{\alpha}{2}) \to t(p,\frac{\sigma}{2})\bar{t}(\bar{p},\frac{\bar{\sigma}}{2})\right)$$
$$= v_\alpha^\dagger(\bar{k})\sigma_\alpha^\mu u_\alpha(k)\sum_{\beta=L,R} A_{\alpha\beta}u_\beta^\dagger(p,\frac{\sigma}{2})\sigma_{\beta\mu}v_\beta(\bar{p},\frac{\bar{\sigma}}{2})$$

$$A_{\alpha\beta} = \frac{-\frac{2}{3}e^2}{q^2} + \frac{g_\alpha^{Zll}g_\beta^{Ztt}}{q^2-m_Z^2}$$



Fierz identities: $\vec{\sigma}_{ij}\cdot\vec{\sigma}_{kl} = 2\delta_{il}\delta_{kj} - \delta_{ij}\delta_{kl}$

$$(\sigma_\pm^\mu)_{ij}(\sigma_{\mp\mu})_{kl} = 2\delta_{il}\delta_{kj}$$
$$(\sigma_\pm^\mu)_{ij}(\sigma_{\mp\mu})_{kl} = 2(\delta_{ij}\delta_{kl} - \delta_{il}\delta_{kj}) = 2(i\sigma^2)_{ik}(i\sigma^2)_{jl}$$

$$M_L^{\sigma\bar{\sigma}} = A_{LL}\left[v_L^\dagger(\bar{k})(i\sigma^2)u_L^*(p,\frac{\sigma}{2})\right]\left[u_L^T(k)(i\sigma^2)v_L(\bar{p},\frac{\bar{\sigma}}{2})\right] + A_{LR}\left[u_R^\dagger(p,\frac{\sigma}{2})u_L(k)\right]\left[v_L^\dagger(\bar{k})v_R(\bar{p},\frac{\bar{\sigma}}{2})\right]$$

In the rest frame of t: t spin is

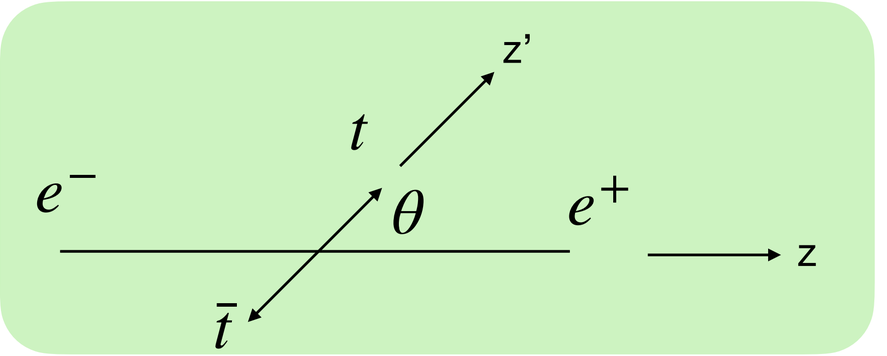
In the rest frame of $\bar{t}$: $\bar{t}$ spin is

} along e^- (opposite of e^+) polarization direction

At the threshold, t rest frame $\sim\bar{t}$ rest frame $\sim e^-e^+$ rest frame

Helicity amplitudes for $e^-e^+ \to t\bar{t}$: non-relativistic limit

$$\begin{cases} M_L^{\pm\mp} = 2E\left\{(A_{LR}+A_{LL})E + (A_{LR}-A_{LL})p\right\}\dfrac{\pm 1-\cos\theta}{2} \\ M_L^{\pm\pm} = 2Em_t(A_{LR}+A_{LL})(\mp\dfrac{\sin\theta}{2}) \end{cases}$$



S-wave ($p \to 0$)

$$\begin{cases} M_L^{\pm\mp} = 2m_t^2(A_{LR}+A_{LL})\dfrac{\pm 1-\cos\theta}{2} \\ M_L^{\pm\pm} = 2m_t^2(A_{LR}+A_{LL})(\mp\dfrac{\sin\theta}{2}) \end{cases} \Rightarrow$$

$$|\uparrow\uparrow\rangle_{z'}\frac{1-\cos\theta}{2} + |\downarrow\downarrow\rangle_{z'}\frac{1+\cos\theta}{2} + \frac{|\uparrow\downarrow\rangle_{z'}+|\downarrow\uparrow\rangle_{z'}}{\sqrt{2}}\frac{\sin\theta}{\sqrt{2}}$$
$$= |\downarrow\downarrow\rangle_z = \Theta\,|j=s=1,\ J_z=m=-1\rangle$$

P-wave linear in p

$$M_L^{\pm\mp} = 2m_t p(A_{LR}-A_{LL})\frac{1\mp\cos\theta}{2} \Rightarrow$$

$$p\left\{|\uparrow\uparrow\rangle_{z'}\frac{1-\cos\theta}{2} - |\downarrow\downarrow\rangle_{z'}\frac{1+\cos\theta}{2}\right\}$$
$$= p\cos\theta\,|\downarrow\downarrow\rangle_z + p\,\frac{\sin\theta}{\sqrt{2}}\,\frac{|\uparrow\downarrow\rangle_z+|\downarrow\uparrow\rangle_z}{\sqrt{2}}$$
$$\sim \chi_t^1\,|j=s=1,\ J_z=m=-1\rangle$$
$$= \frac{|\ell=1,0\rangle_z\,|s=1,-1\rangle_z - |\ell=1,-1\rangle_z\,|s=1,0\rangle_z}{\sqrt{2}}$$

$$r = \frac{p}{m_t}\,\frac{A_{LR}-A_{LL}}{A_{LR}+A_{LL}}$$

Relative strength of P-wave over S-wave

Decay lepton (down-type quark) distribution

$\rho_{m\bar{m},m'\bar{m}'}$

$J_z = m, \bar{m}$

$m\bar{m}$ \ $m'\bar{m}'$	$-+$	$--$	$++$
$-+$	$(1 - r\cos\theta)^2$	$\frac{r}{2}\sin\theta(1 - r\cos\theta)$	$-\frac{r}{2}\sin\theta(1 - r\cos\theta)$
$--$	$\frac{r}{2}\sin\theta(1 - r\cos\theta)$	$\left(\frac{r}{2}\sin\theta\right)^2$	0
$++$	$-\frac{r}{2}\sin\theta(1 - r\cos\theta)$	0	$\left(\frac{r}{2}\sin\theta\right)^2$

$$r = \frac{p}{m_t}\frac{A_{LR} - A_{LL}}{A_{LR} + A_{LL}}$$

$\rho_{m\bar{m},m'\bar{m}'}\rho^{t\to\ell^+}_{mm'}\bar{\rho}^{\bar{t}\to\ell^-}_{\bar{m}\bar{m}'}$

$$\sim (1 - r\cos\theta)^2(1 - \cos\bar{\theta}^*)(1 + \cos\theta^*)$$
$$+ r\sin\theta(1 - r\cos\theta)\left[(1 - \cos\bar{\theta}^*)\sin\theta^*\cos\phi^* - (1 + \cos\bar{\theta}^*)\sin\bar{\theta}\cos\bar{\phi}^*\right]$$
$$+ \left(\frac{r\sin\theta}{2}\right)^2\left[(1 + \cos\bar{\theta}^*)(1 + \cos\theta^*) + (1 - \cos\bar{\theta}^*)(1 - \cos\theta^*)\right]$$

Preliminary

Greens function reweighting of the amplitudes

$$M = M_S + M_P$$

$$\rightarrow \left| \frac{\tilde{G}_S(E,p)}{\tilde{G}_0(E,p)} M_S + \frac{\tilde{G}_P(E,p)}{\tilde{G}_0(E,p)} M_P \right|^2 = \left| \frac{\tilde{G}_S(E,p)}{\tilde{G}_0(E,p)} \right|^2 \left| M_S + \frac{\tilde{G}_P(E,p)}{\tilde{G}_S(E,p)} M_P \right|^2$$

$$M_S \sim 2m_t^2 (A_{LL} + A_{LR}) \,|\downarrow\downarrow\rangle_z$$

$$M_P \sim 2m_t^2 (A_{LL} + A_{LR}) \cdot r \left(-\cos\theta \,|\downarrow\downarrow\rangle_z - \frac{\sin\theta}{\sqrt{2}} \frac{|\downarrow\uparrow\rangle_z + |\uparrow\downarrow\rangle}{\sqrt{2}} \right)$$

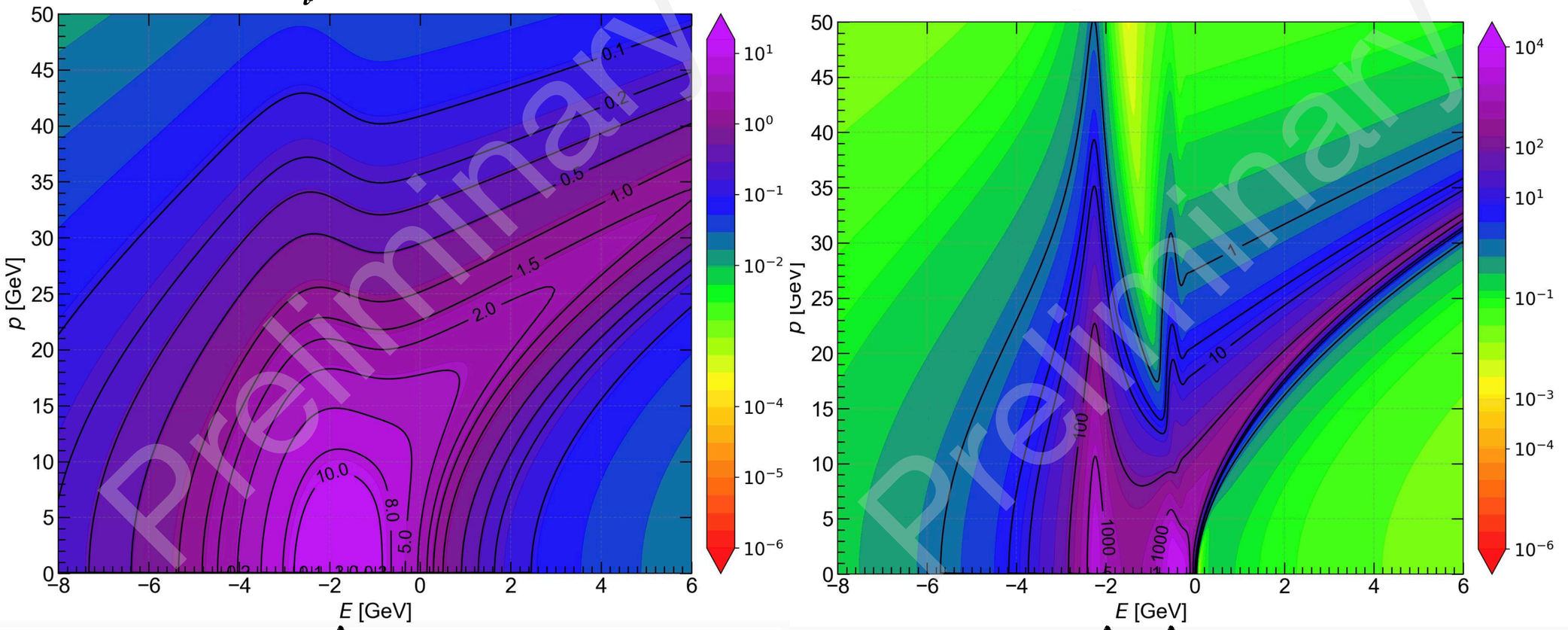
$$\rightarrow 2m_t^2 (A_{LL} + A_{LR}) \left| \frac{\tilde{G}_S(E,p)}{\tilde{G}_0(E,p)} \right|^2 \left| (1 - R\cos\theta) \,|\downarrow\downarrow\rangle_z - \frac{R\sin\theta}{2} \left(|\downarrow\uparrow\rangle_z + |\uparrow\downarrow\rangle_z \right) \right|^2$$

$$r \rightarrow R = \frac{\tilde{G}_P(E,p)}{\tilde{G}_S(E,p)} r = \frac{\tilde{G}_P(E,p)}{\tilde{G}_S(E,p)} \frac{p}{m_t} \frac{A_{LR} - A_{LL}}{A_{LR} + A_{LL}}$$

Both Re(R) and Im(R) can be measured from decay lepton angular correlations.

S-wave Green's Function $|G_s(E,p)|^2$

$\Gamma_t = 1.5\text{GeV}$ → $\Gamma_t = 0.15\text{GeV}$



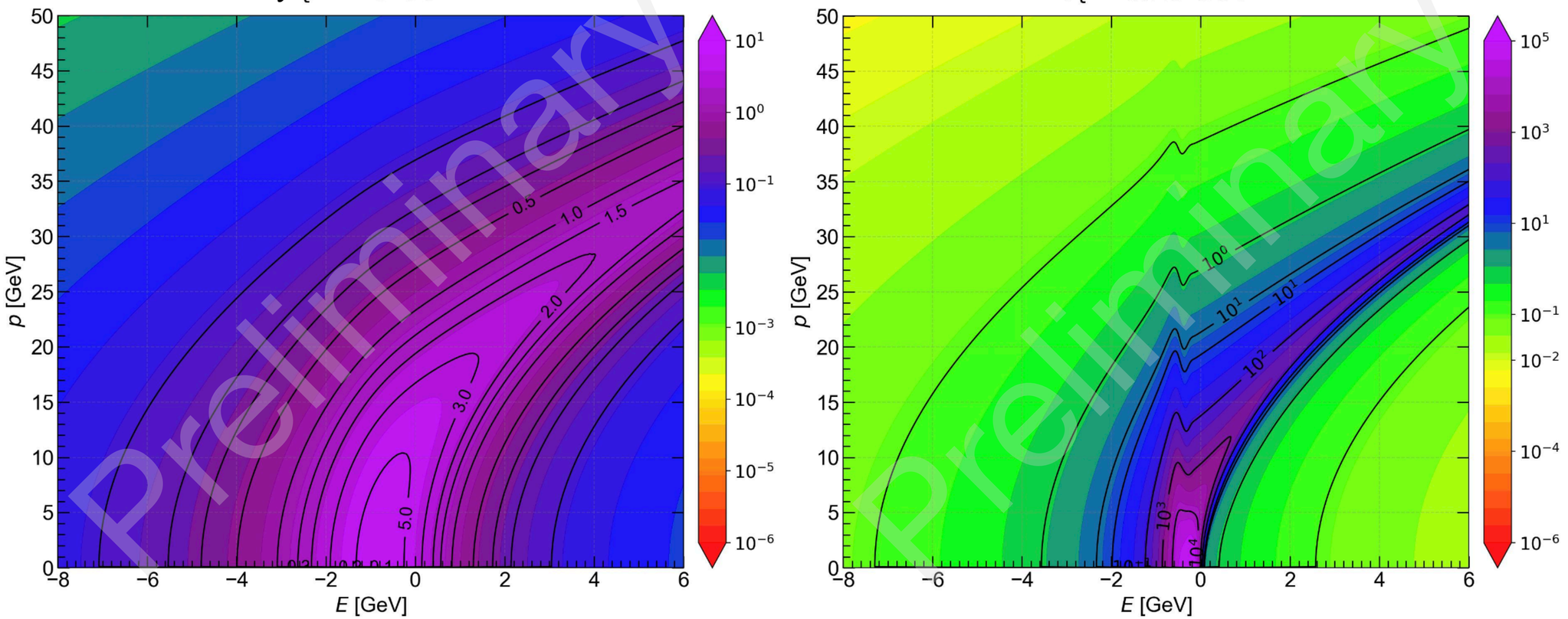
-2GeV

-2GeV -0.5GeV

Preliminary

P-wave Green's Function $|G_P(E,p)|^2$

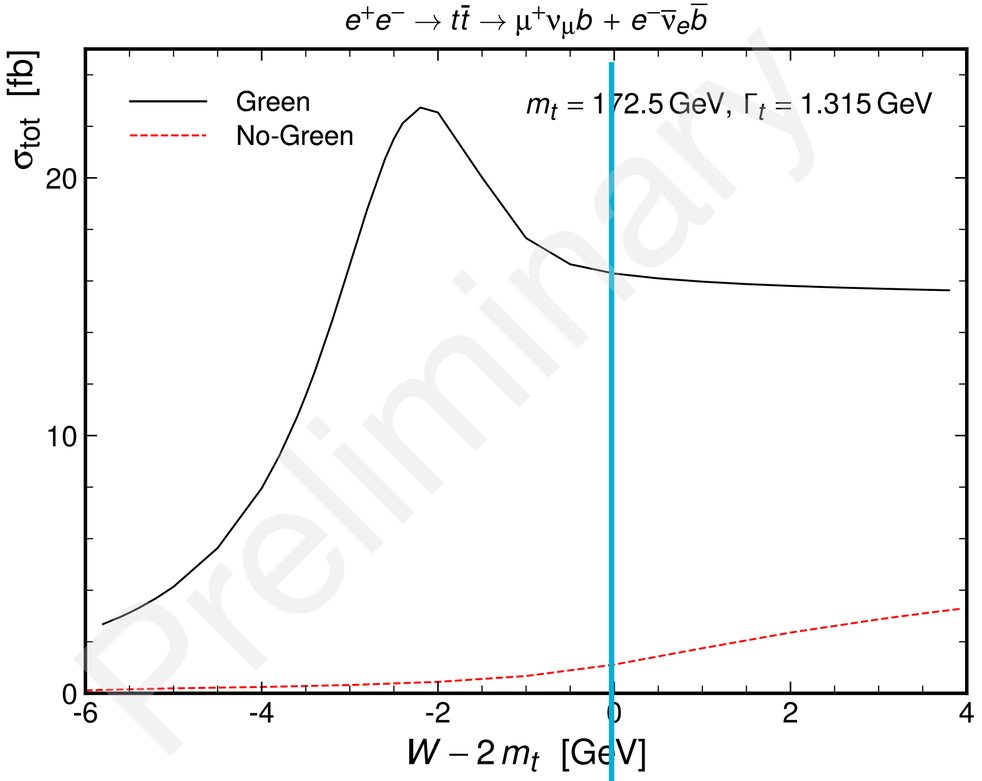
$\Gamma_t = 1.5\text{GeV}$ → $\Gamma_t = 0.15\text{GeV}$

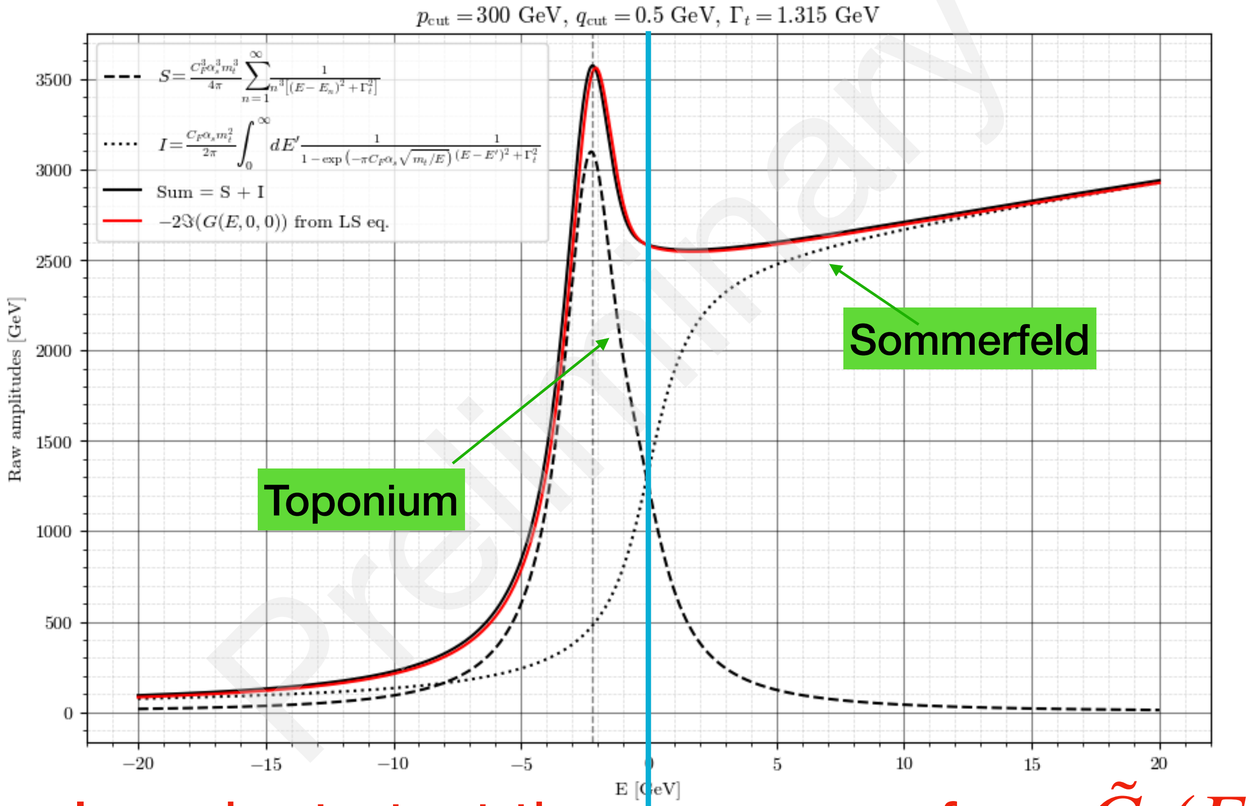


-0.5GeV -0.5GeV

Preliminary

Unitarity $-2ImG_S(E+i\Gamma_t,0) = \int \frac{d^3p}{(2\pi)^3} \left|\tilde{G}_S(E,p)\right|^2 2\Gamma_t$



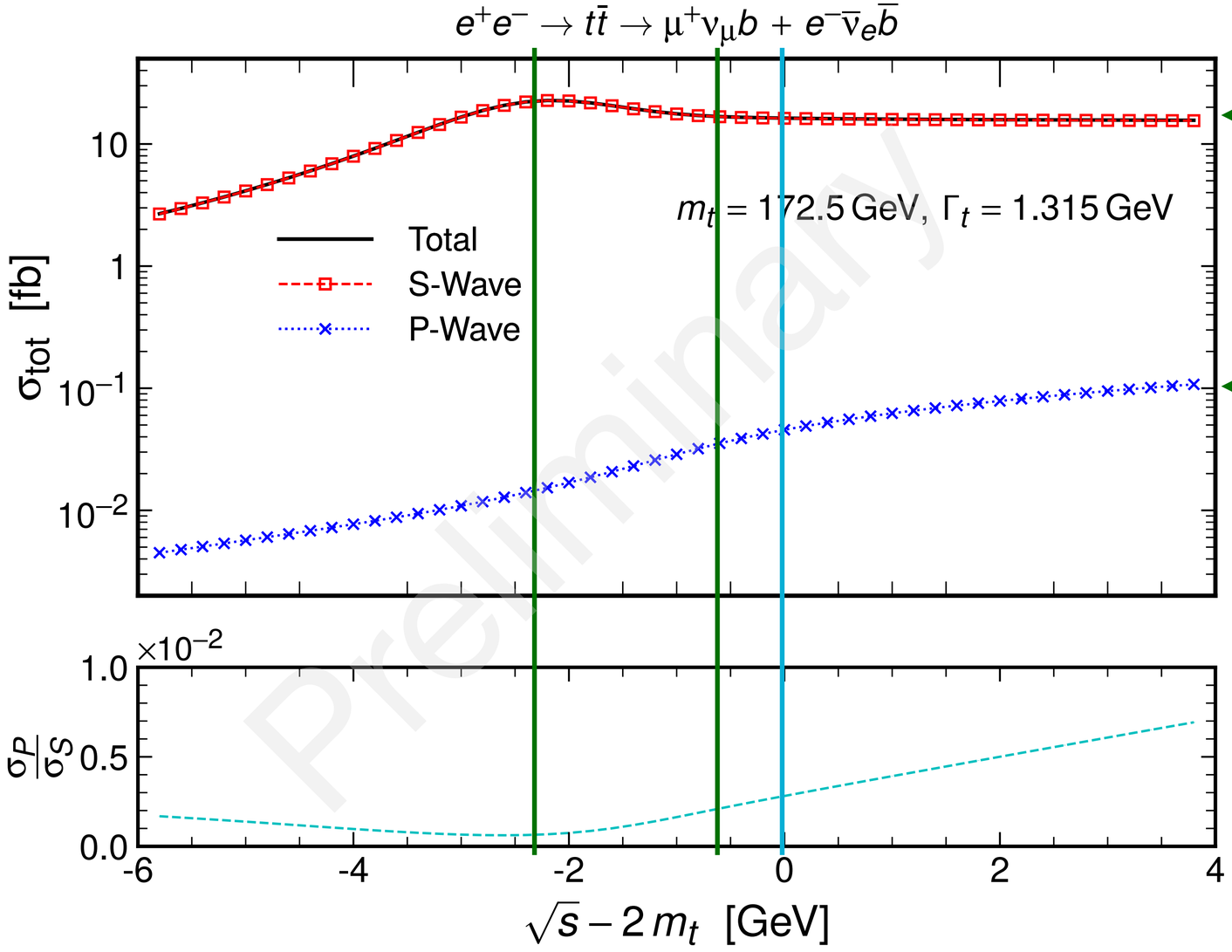


Bound states | Continuum

In order to test the accuracy of our $\tilde{G}_S(E,p)$ by numerically solving the LS equation, we use the Coulomb potential with constant α_S

→ $ImG_S(E+i\Gamma_t,0)$ is known analytically.

Preliminary



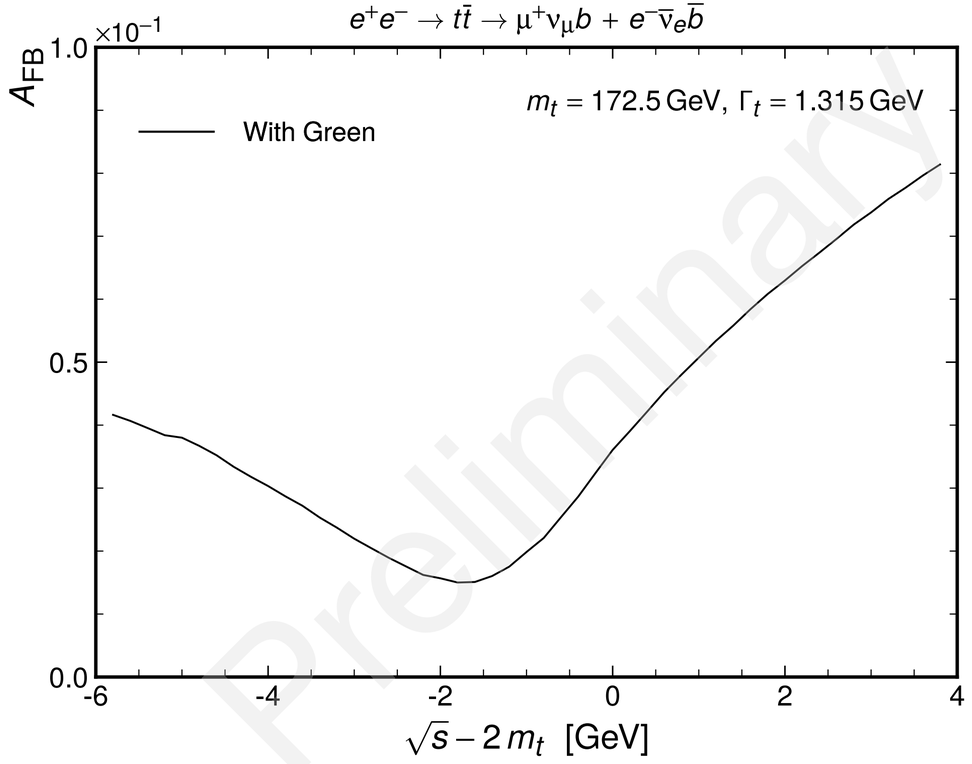
$$\int \frac{d^3p}{(2\pi)^3} \left| \tilde{G}_S(E,p) \right|^2$$

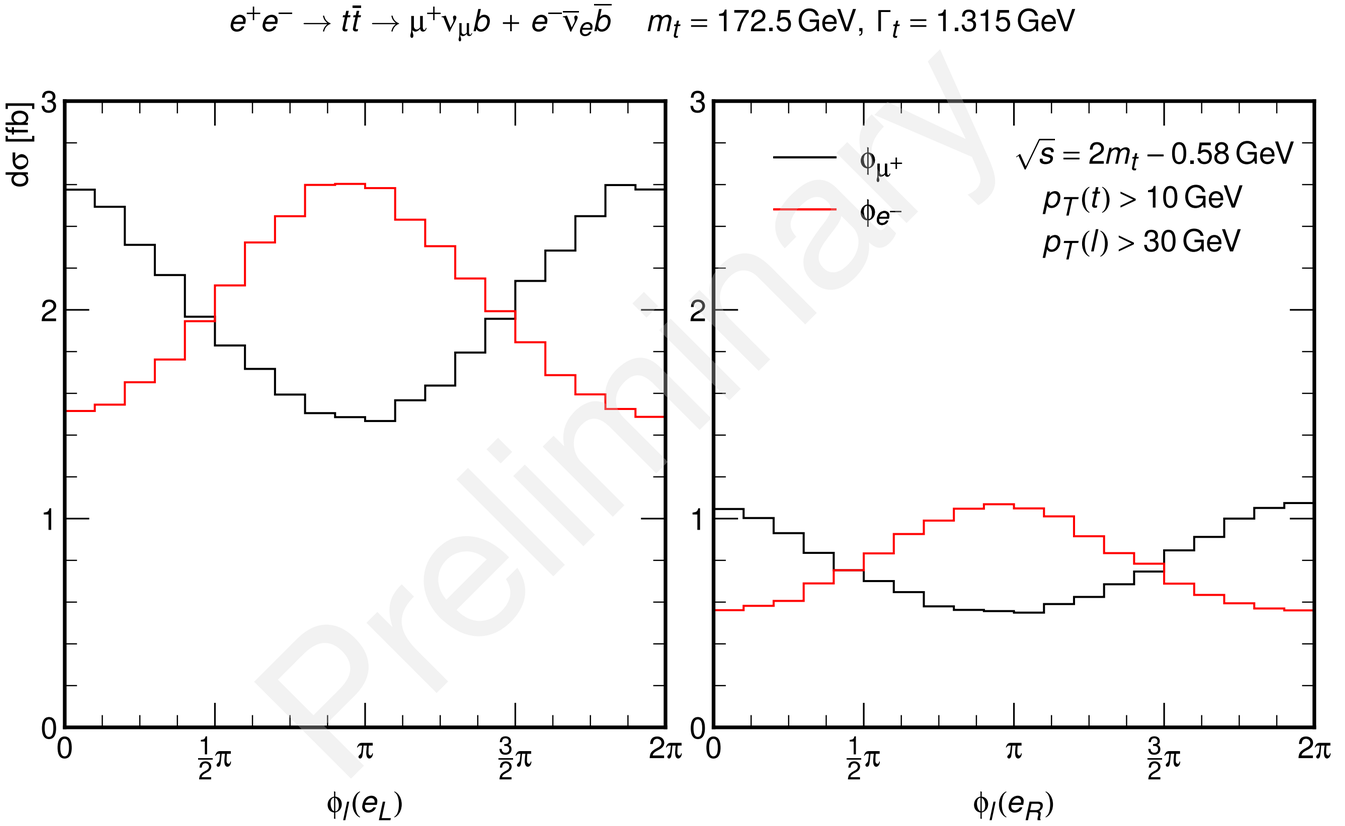
$$\int \frac{d^3p}{(2\pi)^3} \left| \tilde{G}_P(E,p) \right|^2$$

E_1=-2.3GeV E_2=-0.56GeV, no peak at E=-E_2, (χ_t^1)

Preliminary

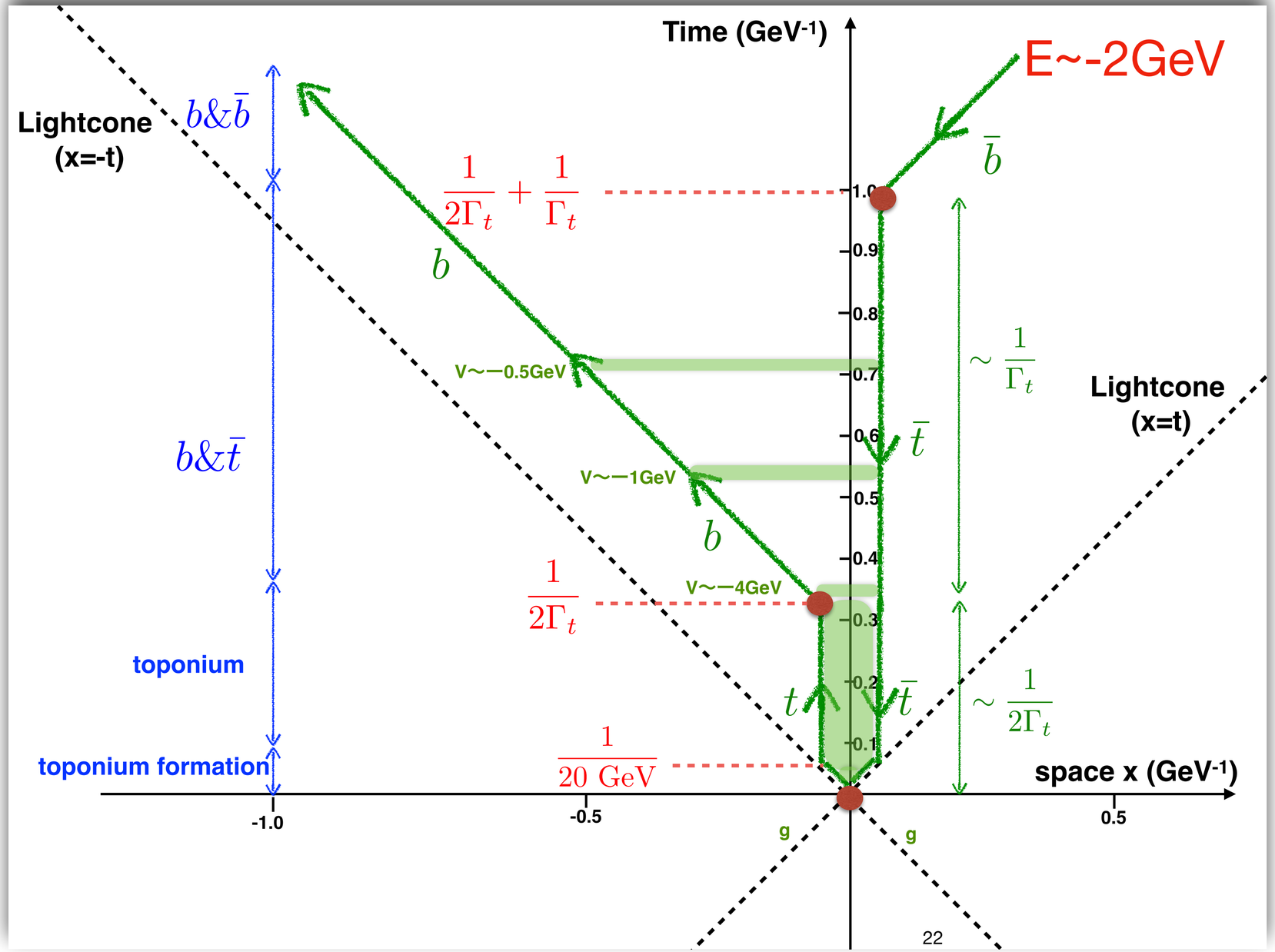
We can discover χ_t^1 by measuring interference between S- and P-wave amplitudes.





H. Murayama, and Y.Sumino, PRD47,82 (1993).

Space-time evolution of toponium formation and decay



- **Coulombic potential**

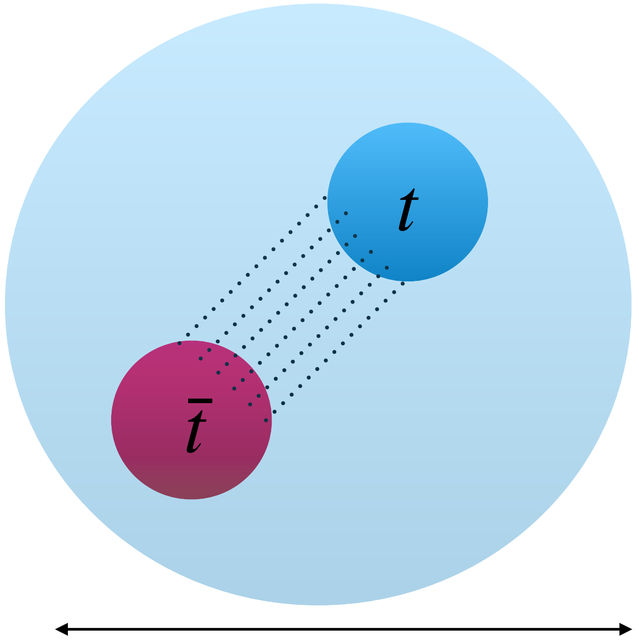
$$V(r) = -\frac{4}{3}\frac{\alpha_S(1/r)_V}{r}$$

- $E_b^{obs.} < E_b^{emis.}$ **not included in our simulation.**

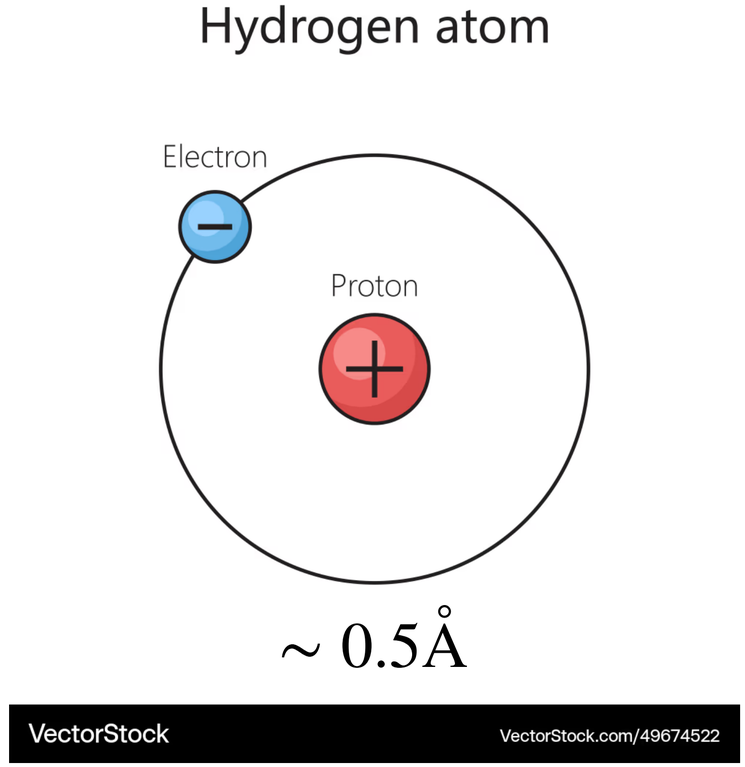
[M.Peter&Y.Sumino, PRD 57,6912 (1998)].

- **P-wave toponium is twice larger than the ground state.**

- We can study quantum physics at the scale of 10^{-7} times smaller than the atoms by using high energy lepton collider, such as ILC.
- Beam polarization is a powerful probe since it directly controls top and anti top spin polarizations.



$$\frac{1}{20\mathrm{GeV}} \sim 0.01fm \sim 10^{-17}m$$



$$1\text{Å} = 0.1nm = 10^{-10}m$$

(Size of positronium)

Backup